

Aalborg Universitet



AALBORG
UNIVERSITY

Optical and AFM study of ion-synthesised silver nanoparticles in thin surface layers of SiO₂ glass

Popok, Vladimir; Gromov, A.V.; Nuzhdin, Vladimir; Stepanov, Andrei

Published in:
Journal of Non-Crystalline Solids

DOI (link to publication from Publisher):
[10.1016/j.jnoncrysol.2010.04.038](https://doi.org/10.1016/j.jnoncrysol.2010.04.038)

Publication date:
2010

Document Version
Publisher's PDF, also known as Version of record

[Link to publication from Aalborg University](#)

Citation for published version (APA):
Popok, V., Gromov, A. V., Nuzhdin, V., & Stepanov, A. (2010). Optical and AFM study of ion-synthesised silver nanoparticles in thin surface layers of SiO₂ glass. *Journal of Non-Crystalline Solids*, 356(25-27), 1258-1261. <https://doi.org/10.1016/j.jnoncrysol.2010.04.038>

General rights

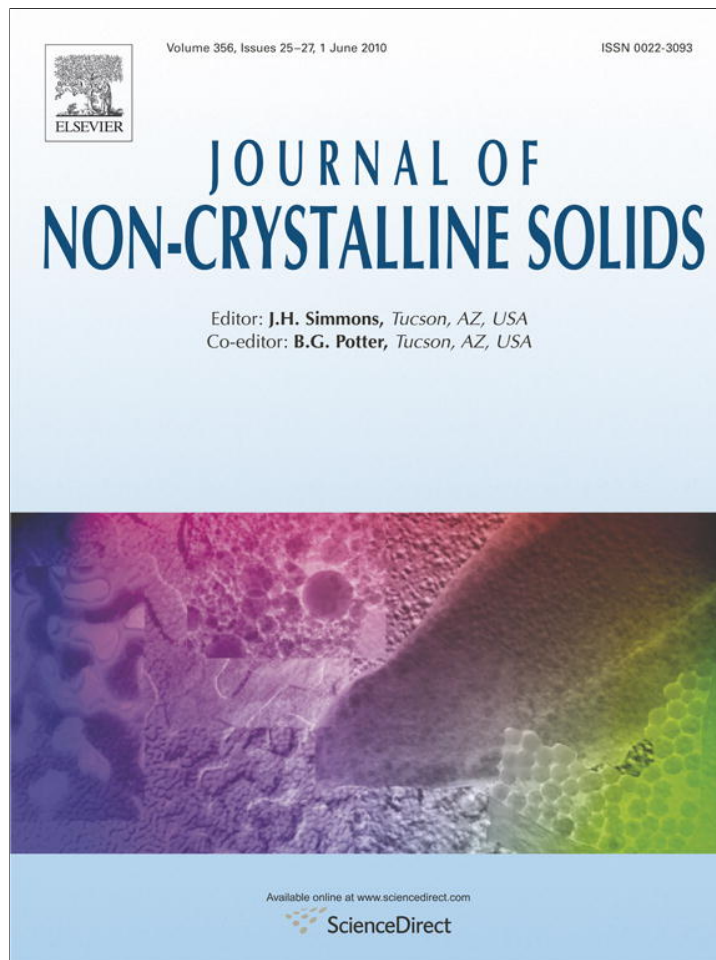
Copyright and moral rights for the publications made accessible in the public portal are retained by the authors and/or other copyright owners and it is a condition of accessing publications that users recognise and abide by the legal requirements associated with these rights.

- Users may download and print one copy of any publication from the public portal for the purpose of private study or research.
- You may not further distribute the material or use it for any profit-making activity or commercial gain
- You may freely distribute the URL identifying the publication in the public portal -

Take down policy

If you believe that this document breaches copyright please contact us at vbn@aub.aau.dk providing details, and we will remove access to the work immediately and investigate your claim.

Provided for non-commercial research and education use.
Not for reproduction, distribution or commercial use.



This article appeared in a journal published by Elsevier. The attached copy is furnished to the author for internal non-commercial research and education use, including for instruction at the authors institution and sharing with colleagues.

Other uses, including reproduction and distribution, or selling or licensing copies, or posting to personal, institutional or third party websites are prohibited.

In most cases authors are permitted to post their version of the article (e.g. in Word or Tex form) to their personal website or institutional repository. Authors requiring further information regarding Elsevier's archiving and manuscript policies are encouraged to visit:

<http://www.elsevier.com/copyright>



Contents lists available at ScienceDirect

Journal of Non-Crystalline Solids

journal homepage: www.elsevier.com/locate/jnoncrysolOptical and AFM study of ion-synthesised silver nanoparticles in thin surface layers of SiO₂ glassV.N. Popok^{a,*}, A.V. Gromov^b, V.I. Nuzhdin^c, A.L. Stepanov^{c,d}^a Department of Physics, University of Gothenburg, 42196 Gothenburg, Sweden^b School of Chemistry, Edinburgh University, West Mains Road, EH9 3JJ Edinburgh, UK^c Kazan Physical-Technical Institute, Russian Academy of Sciences, Sibirsky Trakt 10/7, 420029 Kazan, Russia^d Laser Zentrum Hannover, 30419 Hannover, Germany

ARTICLE INFO

Article history:

Received 5 November 2009

Received in revised form 13 April 2010

Available online 20 May 2010

Keywords:

Ion implantation;

Metal/glass nanocomposite;

Optical spectroscopy;

Atomic force microscopy

ABSTRACT

Silver nanoparticles were synthesised in thin surface layers of SiO₂ glass by 30 keV implantation of Ag⁺ ions with various fluences. Properties of the composites were studied using optical spectroscopy and atomic force microscopy. Optical spectra reveal specific absorption bands assigned to the surface plasmon resonance of the nucleated Ag nanoparticles. The spectral positions of absorption maxima are found to be dependent on the ion fluence that corresponds to the difference in mean sizes of the nanoparticles. Microscopy study shows formation of hemispherical nanosize bumps on the glass surfaces which represent a near-surface fraction of the partly towered nanoparticles. Post-implantation annealing leads to a shift of the plasmon maxima and to a change of the band widths. The transformations of optical spectra are in good agreement with the change of nanoparticle sizes found by atomic force microscopy. Possible mechanisms governing the redistribution of the nanoparticles in size under the thermal treatment are suggested and discussed.

© 2010 Elsevier B.V. All rights reserved.

1. Introduction

High-fluence ion implantation is a well-known way to embed metal species into dielectrics above a solubility limit and to create media with metal nanoparticles (NPs) [1–4]. Depending on metal species, such composite materials can be of interest for nonlinear-optical applications [5–7]. The advantage of ion implantation technique is in the possibility to use practically any combination of substrate material and metal as well as to control the thickness of the doped layer and metal concentration in it. However, the nucleation and growth of metal NPs in any dielectric, for example, glass matrix are complex processes, which strongly depends on implantation parameters such as ion energy, fluence, current density and substrate temperature. One should also consider the radiation damage effects that lead to the modification of initial structure and properties of the dielectric affecting the resulting properties of the composite. Since ion implantation is characterised by statistically non-uniform ion projected ranges, distribution of the embedded metal is not homogeneous in the implanted layer both in the plane parallel to the surface and in the depth [2,8,9]. Such non-homogeneity leads to

broad distribution of the NPs in size that can have a negative effect for some applications. On the other hand, media with non-uniformly size distributed metal NPs can be used for construction of optical dichroic mirrors and Fabry–Perot resonators [10].

It was shown that post-implantation thermal annealing can be a method to change a size distribution of NPs [11–16]. Also, laser pulse annealing can be effectively applied for the size modification of NPs [17]. For example, high power pulsed laser irradiation was used for annealing of the Cu-implanted sapphire that led to the decrease of a mean size of the copper NPs [18]. Similar effect was observed for silver NPs in glass [19]. Moreover, the combination of laser and furnace annealing allowed the improvement of the size uniformity. However, physics of the phenomena leading to shrinkage or enlargement of metal NPs in size under the heating is rather complex. On the one hand, it depends on used metal species, size of NPs, their concentration and a distribution in host matrix as well as on the composition and structure of latter one. On the other hand, the specific temperature conditions during the annealing process strongly affect a modification of the composite material. Thus, a development of optimal regimes for synthesis of metal/dielectric composites with required parameters is still a topical research area.

In this paper new data on optical properties of ion-synthesised silver NPs in SiO₂, which are considered in consistence with the atomic force microscopy (AFM) measurements of surface topography, are presented. Additionally, post-implantation furnace annealing is used to control size distribution of the synthesised NPs.

* Corresponding author. Current address: Institut für Physik, Universität Rostock, Universitätsplatz 3, 18051 Rostock, Germany. Tel.: +49 381 4986804; fax: +49 381 4986802.

E-mail address: vladimir.popok@uni-rostock.de (V.N. Popok).

2. Experimental

Quartz glasses SiO₂ (Heraeus) with thickness of 1 mm were implanted by 30 keV Ag⁺ ions with fluences in the range of 7.5×10^{15} – 1.0×10^{17} cm⁻² at ion current density of 4 μA/cm² in residual vacuum of 10⁻⁵ Torr using ion accelerator ILLU-3 [20,21]. The sample holder was water-cooled to prevent glass overheating during the implantation. Optical absorption of the Ag:SiO₂ composites was studied using the UV–visible range fibre optic spectrometer (Ocean Optics, model USB2000) in the wavelength interval from 350 to 850 nm where the transparency of pristine glass was about 92%. Surface topography of the implanted samples was studied by AFM in tapping mode using Ntegra Aura Probe NanoLaboratory from NT-MDT. Commercial Si cantilevers with curvature radius of about 10 nm were used. Additionally, the implanted samples were annealed in furnace at 300 °C for 1 h in inert Ar atmosphere. After the annealing, optical properties and surface topography were studied again and compared with the as-implanted samples.

3. Results

Modelling of 30 keV Ag⁺ ion implantation into SiO₂ substrate using SRIM-2008 [22] gives a mean projected range of ions 23.5 ± 6.0 nm. However, it is very well known that in the case of low-energy (<ca. 100 keV) and high-fluence (>ca. 10¹⁶ ion/cm²) ion bombardment of dielectrics the experimental impurity depth profiles significantly deviate from the simulated by SRIM ones due to a number of effects which are not taken into account in this simple code such, for instance, as a diffusion of the implanted atoms, change of the target composition and sputtering of the irradiated surface [20]. All these effects lead to a broadening of the impurity depth profile and to the shift of concentration maximum towards the surface. Thus, if we consider that most of implanted silver ions in our case accumulate in ca. 50 nm thick surface layer then silver atomic concentration can reach a value of about 2.0×10^{21} cm⁻³ for the fluence of 1.0×10^{16} cm⁻² that is much higher than the silver solubility limit in solid SiO₂ at room temperature (3×10^{18} cm⁻³ [23]). It is well known that embedding of metal atoms in glass by implantation above the solubility threshold leads to nucleation and growth of NPs [2].

The further increase of ion fluence above 1.0×10^{16} cm⁻² causes considerable sputtering of the surface that in turn originates shift of the final impurity depth profile towards surface [28,29]. Thus, maximum of the silver distribution can be located just about 10 nm below the surface level and the concentration monotonically decreases towards bulk. Effective accumulation of silver atoms just beneath the surface should lead to the formation of shallow-located NPs as schematically shown in Fig. 1. These particles are typically spherical in shape [2]. One should also take into account that ion sputtering rate is different for various materials. For instance, SRIM-2008 code shows that sputtering rate for Ag atoms incorporated during the implantation into SiO₂ matrix is a few times lower compared to both Si and O sputtering rates [22]. Therefore, at later stage of higher fluence implantation, incoming Ag⁺ ions efficiently sputter the surface layer of SiO₂ that causes towering above the

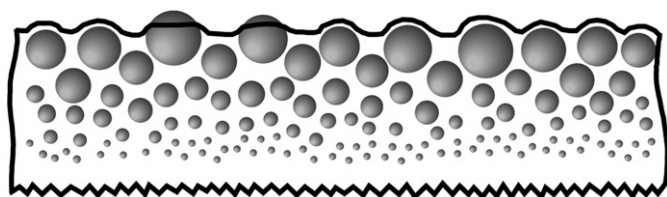


Fig. 1. Schematic picture of NP nucleation and towering above the surface level under high-fluence low-energy implantation.

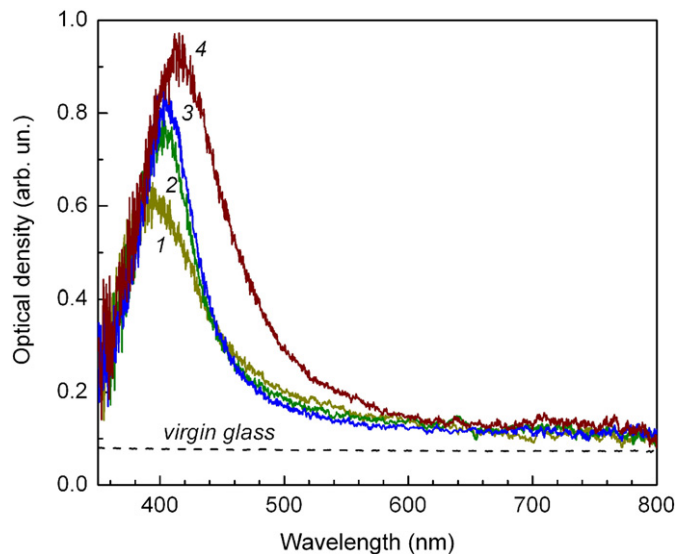


Fig. 2. Optical absorption spectra of samples implanted with fluences of (1) 0.75×10^{16} , (2) 2.5×10^{16} , (3) 5.0×10^{16} and (4) 1.0×10^{17} cm⁻². Spectrum of virgin glass is presented as dashed line.

surface of already nucleated (at earlier stage of implantation) very shallow-located Ag NPs. This scenario was experimentally proved earlier for different combinations of metal ions and dielectric substrates [28,31,24].

Fig. 2 presents optical spectra of the glass substrates implanted with different fluences of Ag⁺ ions. All spectra demonstrate characteristic absorption band with maximum at around 400 nm. This location of the band on the wavelength scale is typical for plasmon resonance of Ag NPs [25]. One can see that the fluence increase leads to (i) the increase of absorption intensity, (ii) gradual shift of the absorption maximum towards longer wavelengths and (iii) broadening of the absorption band at the highest fluence. Similar tendencies for optical plasmon resonance spectra were found earlier for some other ion-synthesised metal/dielectric composites [8,26].

In panels (a–c) of Fig. 3 one can see AFM images of the glass surfaces after the ion implantation with different fluences of Ag⁺ ions. All images show surface bumps of nanometer sizes related to the towered NPs in consistence with the above-presented consideration. Hemispherical shape of the bumps reflects a top part of spherical NPs. It should be noted that surface of glass before implantation was found to be smooth (roughness of ca. 0.5 nm for scan areas of 2×2 μm) without any bumps or protrusions. Unfortunately, the AFM imaging cannot be used for direct quantitative measurements of the NP sizes because of two main reasons. The first one is an enlargement of the lateral dimensions of the nano-scale features due to the AFM tip convolution [27], because the tip curvature radius is of the same order as NP size. The second one is uncertainty in how large part of the NP is towered above the glass surface level.

Optical absorption spectra of the implanted samples after the thermal annealing are presented in Fig. 4. Compared to as-implanted samples (Fig. 2), spectral shifts of the absorption maxima and some changes in plasmon band width for selected fluences are observed (Table 1). For the lowest fluence (7.5×10^{15} cm⁻²), there is a pick shift to the longer wavelength from 395 to 400 nm but there is no change (within the measurement uncertainty) of the band width. For higher fluences (2.5×10^{16} , 5.0×10^{16} and 1.0×10^{17} cm⁻²), one can see the shift of the absorption maxima to shorter wavelengths and inhomogeneous broadening of the absorption bands: the short-wavelength wings (on the left-hand side of spectral curves 2–4 in Fig. 4) of the bands remain unchanged in width while long-wavelength wings (on the right-hand side) become much broader after the annealing.

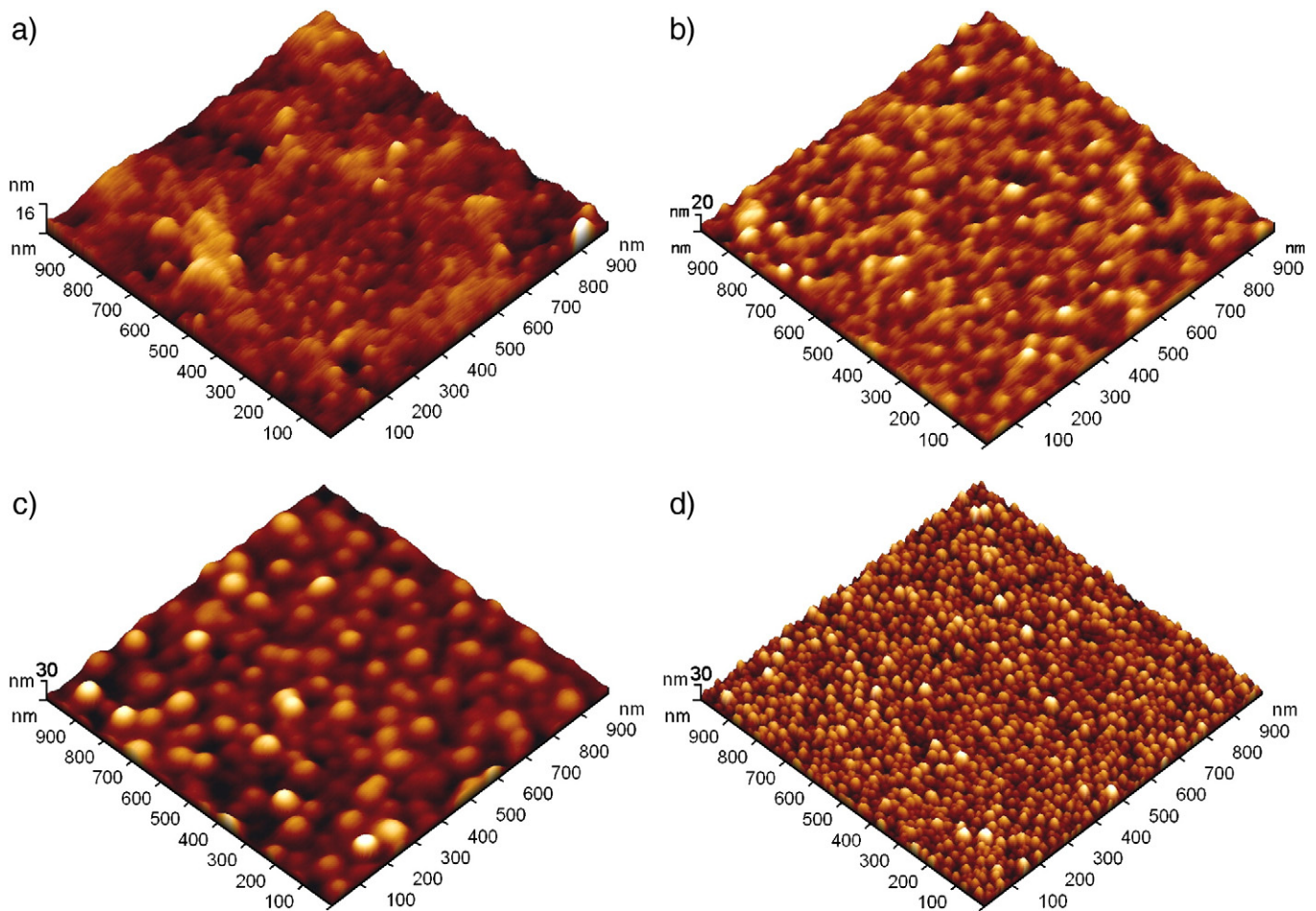


Fig. 3. AFM images of samples implanted with fluences of (a) 0.75×10^{16} , (b) 2.5×10^{16} , and (c) $5.0 \times 10^{16} \text{ cm}^{-2}$. Image (d) shows case of fluence of $5.0 \times 10^{16} \text{ cm}^{-2}$ after thermal annealing.

4. Discussion

The rise of absorption intensity with fluence shown in Fig. 2 is related to the increased concentration of silver in the implanted layer that causes higher density of the NPs. Second effect demonstrating shift of the plasmon band maximum from ca. 395 nm to 415 nm (see Table 1)

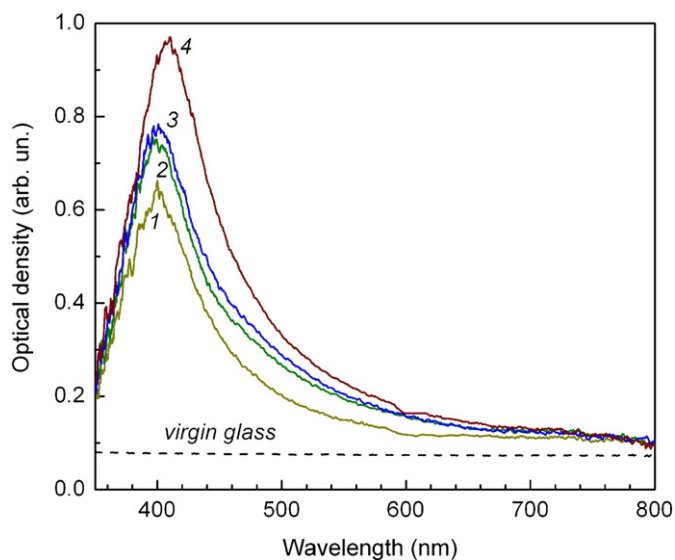


Fig. 4. Optical absorption spectra of samples implanted with fluences of (1) 0.75×10^{16} , (2) 2.5×10^{16} , (3) 5.0×10^{16} and (4) $10 \times 10^{16} \text{ cm}^{-2}$ after thermal annealing.

corresponds to the increase of average size of the NPs that follows from the consideration of the Mie theory [30]. The observed changes of the band width are related to some variations of size dispersion of the nucleated NPs for different fluences. Consecutive embedding of metal to very high concentration by implantation into glass matrix can lead not only to the growth of already formed NPs but also to the efficient formation of new nucleation sites for NPs due to the introduced radiation defects. This situation typically causes quite broad distribution of the synthesised NPs in size [25]. However, we do not exclude a possibility that competition of several phenomena related to nucleation of NPs, their growth and formation of radiation damage can cause fluctuations of size dispersion for certain fluencies. However, we should emphasize that the general tendency is the increase of both mean sizes and size distribution at high fluencies (Table 1).

From the AFM images in Fig. 3 it is clearly seen that size of the bumps increases with rise of ion fluence in agreement with the tendency found from the optical absorption spectra (Fig. 2). Thus, both optical and AFM

Table 1

Dependence of maxima and widths of absorption bands on ion fluence before and after annealing.

Fluence, cm^{-2}	As-implanted		Annealed	
	Maximum, nm	Band width, nm	Maximum, nm	Band width, nm
7.5×10^{15}	395	86	400	88
2.5×10^{16}	405	80	400	98
5.0×10^{16}	407	74	400	105
1.0×10^{17}	415	99	410	107

measurements provide evidence for the formation of larger NPs at higher ion fluences. This observation is consistent with our earlier comparisons of AFM and optical study of Ag NP synthesis in SiO₂ at different ion current densities [32]. Therefore, AFM analysis can be suggested as an effective technique for qualitative estimation of sizes of NPs fabricated by low-energy implantation.

Annealing of the samples at 300 °C causes significant changes in both optical absorption spectra (see Table 1) and AFM images. For the smallest fluence, the mean size of the NPs is just slightly increased that can be explained by thermally enhanced diffusion of silver atoms spread in the implanted layer towards the already existing NPs. Additionally, the heating can cause melting and dissociation of the smallest NPs which have quite low melting temperatures [33], then the realised silver atoms contribute into the growth of larger particles.

The shifts of plasmon maximum to shorter wavelengths in the spectra 2–4 presented in Fig. 4 can be explained as a decrease of mean size of the Ag NPs [25]. On the other hand, the broadening of the long-wavelength part of the band is probably related to the increase of fraction of larger particles in the total size distribution. Such changes in both the mean particle size and size dispersion can be interpreted in the following way. The heating causes dissociation of the smallest NPs and enhanced diffusion of the spread silver atoms. These silver atoms can contribute into the growth of larger NPs which is a dominant process under the surface leading to the broadening of the long-wavelength part of the absorption band. On the other hand, the AFM images show that the fraction of the NPs towered above the surface has tendency to decrease in size after the annealing as, for example, can be seen from comparison of Fig. 3c and d. Similar changes in surface morphology are observed for other high fluences ($2.5 \times 10^{16} \text{ cm}^{-2}$ and $1.0 \times 10^{17} \text{ cm}^{-2}$). This decrease in size is most probably caused by partial dissociation of the near-surface located NPs followed by sublimation of silver. However, this sublimation does not lead to significant decrease of silver concentration in the near-surface layer due to relatively low annealing temperature [34]. Thus, we believe that the above-mentioned mechanisms of NP rearrangement are responsible for both the shift of the plasmon maxima and the broadening of the long-wavelength part of the bands.

5. Conclusions

Silver nanoparticles were synthesised in shallow layers of quartz glass using low-energy (30 keV) high-fluence ion implantation. Optical spectroscopy of the ion-implanted samples shows the appearance of specific absorption bands assigned to plasmon resonance of the silver nanoparticles. Spectral positions of the absorption maxima shift towards longer wavelength with the increase of ion fluence that corresponds to enlargement of the NPs. AFM study shows formation of the hemispherical nanosize bumps on the glass surfaces. The bumps represent a shallow-located fraction of the NPs which are partly towered above the surface level. Good correlation between the increase of the bump sizes and the spectral shift of the optical absorption bands with increasing fluence is found. Thus, AFM can be suggested as efficient tool for qualitative size analysis of the very shallow-located ion-synthesised NPs. Post-implantation thermal annealing at 300 °C causes the size redistribution of the NPs. The general tendency found for the high fluencies is the decrease in mean particle size and the increase in size dispersion. Two different processes governing the change of the NPs

in size under thermal treatment are suggested: one for the bulk fraction of the particles and another one for the surface fraction. Careful consideration of possible mechanisms of NP nucleation, growth or dissociation is of significant importance for synthesis of nanoparticulate materials with required properties.

Acknowledgements

One of the authors (V.N.P.) is grateful to the Swedish Research Council for the partial financial support of these studies. A.L.S. is grateful to the Alexander von Humboldt Foundation (Germany). He also acknowledges the support of Russian State Contract No. 02.740.11.0797.

References

- [1] E. Cattaruzza, F. Gonella, in: H.S. Nalwa (Ed.), *Encyclopedia of Nanoscience and Nanotechnology*, vol. 5, Amer. Sci. Publ, 2004, p. 369.
- [2] A.L. Stepanov, in: D.P. Perez (Ed.), *Silver Nanoparticles*, In-Tech, Vukovar, 2010, p. 93.
- [3] A.L. Stepanov, V.N. Popok, D.E. Hole, *Glass Phys. Chem.* 28 (2002) 90.
- [4] V.N. Popok, R.I. Khaibullin, A. Toth, V. Beshliu, V. Hnatowicz, A. Mackova, *Surf. Sci.* 532–535 (2003) 1034.
- [5] A. Meldrum, R.F. Haglund Jr., L.A. Boatner, C.W. White, *Adv. Mater.* 13 (2001) 1431.
- [6] A.I. Rysanyanskiy, B. Palpant, S. Debrus, U. Pal, A.L. Stepanov, *Opt. Comm.* 127 (2007) 181.
- [7] Y. Takeda, O.A. Plaksin, N. Kishimoto, *Opt. Express* 15 (2007) 6010.
- [8] L.C. Nistor, J. van Landuyt, J.D. Barton, D.E. Hole, N.D. Skelland, P.D. Townsend, *J. Non.-Cryst. Sol.* 162 (1993) 217.
- [9] N. Kishimoto, N. Umeda, Y. Takeda, C.G. Lee, V.T. Gritsyna, *Nucl. Instr. Meth. Phys. Res. B* 148 (1999) 1017.
- [10] R.H. Magruder III, S.J. Robinson, C. Smith, A. Meldrum, A. Halabica, R.F. Haglund Jr., *J. Appl. Phys.* 105 (2009) 024303.
- [11] N. Umeda, N. Kishimoto, Y. Takeda, C.G. Lee, V.T. Gritsyna, *Nucl. Instr. Meth. Phys. Res. B* 166–167 (2000) 864.
- [12] R.A. Wood, P.D. Townsend, N.D. Skelland, D.E. Hole, J. Barton, C.N. Afonso, *J. Appl. Phys.* 74 (1993) 5754.
- [13] A. Miotello, G. de Marchi, G. Mattei, P. Mazzoldi, C. Sada, *Phys. Rev. B* 63 (2001) 75409.
- [14] J. Roiz, A. Oliver, E. Munoz, L. Fernandez-Rodriguez, J.M. Hernandez, J.C. Cheng-Wong, *J. Appl. Phys.* 95 (2004) 1783.
- [15] L.H. Zhou, C.H. Zhang, Y.T. Yang, B.S. Li, L.Q. Zhang, Y.C. Fu, H.H. Zhang, *Nucl. Instr. Meth. Phys. Res. B* 267 (2009) 58.
- [16] J.-X. Xu, F. Ren, D.-J. Fu, C.-Z. Jiang, *Physica B* 373 (2006) 341.
- [17] A.L. Stepanov, in: A.L. Stepanov (Ed.), *High-power and Femtosecond Lasers: Properties, Materials and Applications*, Nova Sci. Publ, New York, 2009, p. 34.
- [18] A.L. Stepanov, V.N. Popok, D.E. Hole, I.B. Khaibullin, *Appl. Phys. A* 74 (2002) 441.
- [19] A.L. Stepanov, V.N. Popok, *Surf. Coat. Technol.* 185 (2004) 30.
- [20] A.L. Stepanov, I.B. Khaibullin, *Rev. Adv. Mater. Sci.* 9 (2005) 109.
- [21] J. Gyulai, *Nucl. Instr. Meth. Phys. Res. B* 267 (2009) 1217.
- [22] J.F. Ziegler, J.P. Biersack, M.D. Ziegler, *The stopping and ranges of ions in matter*, Lulu Press, Morrisville, 2008.
- [23] J.D. McBrayer, R.M. Swanson, T.W. Sigmon, *J. Electrochem. Soc.* 133 (1986) 1242.
- [24] M.T. Pham, W. Matz, W. Seifarth, *Anal. Chim. Acta* 350 (1997) 209.
- [25] A.L. Stepanov, V.A. Zhikharev, I.B. Khaibullin, *Phys. Sol. State* 43 (2001) 776.
- [26] A.A. Bukharaev, V.M. Janduganov, E.A. Samarsky, N.V. Berdunov, *Appl. Surf. Sci.* 103 (1996) 49.
- [27] V.N. Popok, A.L. Stepanov, V.B. Odzhaev, *J. Appl. Spectrosc.* 72 (2005) 229.
- [28] U. Kreibig, in: R.E. Hummel, P. Wissmann (Eds.), *Handbook of Optical Properties*, vol. 2, CRC Press, Boca Raton, 1997, p. 145.
- [29] Z. Liu, Hao Li, X. Feng, S. Ren, H. Wang, Z. Liu, B. Lu, *J. Appl. Phys.* 84 (1998) 1913.
- [30] A.A. Bukharaev, N.V. Berdunov, D.V. Ovchinnikov, K.M. Salikhov, *Scan. Microsc.* 12 (1998) 225.
- [31] C.F. Boren, D.R. Huffman, *Absorption and scattering of light by small particles*, Wiley Sons, New York, 1983.
- [32] A.L. Stepanov, V.N. Popok, *Surf. Sci.* 566–568 (2004) 1250 and references therein.
- [33] T. Castro, R. Reifenberger, E. Choi, R.P. Andres, *Phys. Rev. B* 42 (1990) 8548.
- [34] P.D. Townsend, P.J. Chandler, L. Zhang, *Optical Effects of Ion Implantation*, Cambridge University Press, Cambridge, 1994.